IOSR Journal of Applied Geology and Geophysics (IOSR-JAGG)
e-ISSN: 2321–0990, p-ISSN: 2321–0982.Volume 6, Issue 5 Ver. I (Sep. – Oct. 2018), PP 44-55
www.iosrjournals.org

Inferring Groundwater Types From Graphical Methods: A Case Study of Afikpo And Abakaliki, South-Eastern Nigeria

Mgbeojedo T.I[1], Al-Naimi L.S[2], Nosiri O.P[3]
[1](Professional Founder Geological Consulting, Al Gharafa, Doha, Qatar)
[2](Department of Chemistry and Earth Sciences, Qatar University, Doha, Qatar)
[3](Department of Geosciences, Federal University of Technology, Owerri, Nigeria)
Corresponding author: Mgbeojedo T.I[1]

Abstract: *The chemical composition of surface and groundwater is controlled by many factors that include composition of precipitation, mineralogy of the watershed and aquifers, climate, and topography. These factors combine to create diverse water types that change spatially and temporally. In our study area which lies within the Cross River Basin, there is a wide variety of climatic conditions, hydrologic regimes (alluvial basin-fill aquifers, fractured rock aquifers, etc) and geologic environments (igneous rocks, volcanic rocks, metamorphic rocks, sedimentary deposits, evaporites, and mineralized zones). Thus, the samples from the area could potentially represent a variety of water types providing an opportunity to test the performance of many of the available graphical and statistical methodologies used to classify water samples. Generally, the approach is to divide the samples into hydrogeochemical facies (water types), that is groups of samples with similar chemical characteristics that can then be correlated with location. The spatial variability observed in the composition of these natural tracers can provide insight into aquifer heterogeneity and connectivity, as well as the physical and chemical processes controlling water chemistry. Stiff diagrams, Piper trilinear plots and Schoeller diagrams were used to determine the hydrogeochemical facies of the study area. From the plots, three major water types were identified in the study area, viz: Na–K–Cl–SO_4–HCO_3, Na–K–HCO_3–Cl–SO_4,and Na–Ca–Cl–SO_4–HCO_3^- water types. The water types tend towards sodium chloride bicarbonate which is consistent with expected water-rock interactions in the area.*

Keywords: *Hydrogeochemical facies, water chemistry, graphical methods, Cross river basin, aquifer heterogeneity*

Date of Submission: 14-09-2018 Date of acceptance: 29-09-2018

I. Introduction

A variety of graphical and multivariate statistical techniques have been devised since the early 1920's in order to facilitate the classification of waters, with the ultimate goal of dividing a group of samples into similar homogeneous groups (each representing a hydrogeochemical facies). Several commonly used graphical methods and multivariate statistical techniques are available including: Collins bar diagram, pie diagram, Stiff pattern diagram, Schoeller semi-logarithmic diagram, Piper diagram, Q-mode hierarchical cluster analysis (HCA), K-means clustering (KMC), Principal components analysis (PCA) and Fuzzy k-means clustering (FKM). This work utilizes a relatively large data set to review these techniques and compare their ease of use and ability to sort water chemistry samples into groups. But for the purpose of this study only the following techniques were used: Stiff Diagram, Piper Diagram and Schoeller Semi-logarithmic Diagram.

Geochemical study is very important and helps in understanding the hydrogeologic system.

It also helps to indicate the commingling of groundwater and surface water thereby aiding in studying groundwater flow dynamics. This may include the determination of possible source/origin of groundwater. The origin/source of the water may include the following: meteoric water (water from precipitation), which is generally high in carbonate ions and low in dissolved solids. pH is usually neutral; however, sulphur emissions have been shown to reduce pH. The origin may also be primary or juvenile water (formed chemically within the earth and brought to the surface in intrusive rock) which is generally high in dissolved solids and sulphur. Geochemical studies may also be used to delineate groundwater contamination.

Most of the graphical methods are designed to simultaneously represent the total dissolved solid concentration and the relative proportions of certain major ionic species[5]. All the graphical methods use a limited number of parameters, usually a subset of the available data, unlike the statistical methods that can utilize all the available parameters. The fundamental aim of the techniques compared here is to identify the chemical relationships between water samples. Samples with similar chemical characteristics often have similar

hydrologic histories, similar recharge areas, infiltration pathways, and flow paths in terms of climate, mineralogy, and residence time.

Geological/hydrogeological setting

The study area is within the Benue Trough. The general geology and stratigraphy of the southern portion of the Benue Trough has been described by several authors and is therefore sufficiently understood[7,9]. The oldest sediment in the study area belongs to the Asu River group which uncomfortably overlies the Precambrian basement complex that is made up of granitic and magmatic rocks. The Asu River Group whose type section outcrops near Abakaliki and has an estimated thickness of 2000m[9]and is of Albian age. It comprises of argillaceous sandy shales, laminated sandstones, and micaceous sandstones and limestones with an interfingering of mafic volcanics. It is associated with pyrosclastic roles especially around Abakaliki and Eziulor areas[13,8,6]. Deposited on top of the Asu River Group sediments in the area are the upper cretaceous sediments, comprising mostly of the Ezeaku shales which consists of nearly 1000m of calcareous flaggy shales and siltstones, thin sandy shaley limestones and calcareous sandstones[12]. They are of Turonian age and are overlain by the younger sediments of the Awgu shale (Coniacian). The Awgu shales consists of marine fossiliferous grey blue shales, limestones and calcareous sandstones.They are overlain by the Nkporo shales (Campanian) which are also mainly marine in character and has sandstone members.

The Afikpo area consists of two major lithostratigraphic units of sandstone ridges and low-lying shales, each of which forms significant component of the Middle Albian Asu River Group and Turonian Ezeaku Formation. The major folds in the area have northeast-southwest trend, and comprise both anticlines and synclines. These mega-tectonic structures developed in response to crustal solidification processes linked to the opening of the South Atlantic and the post-Santonian structural framework as a result of these processes[14].

The study area is located within the Cross River Basin hydrological province which is known as a problematic groundwater basin. The geology, geomorphology, sedimentology and hydrogeology of the Cross River basin have been extensively studied by several authors[4,2,3,1].

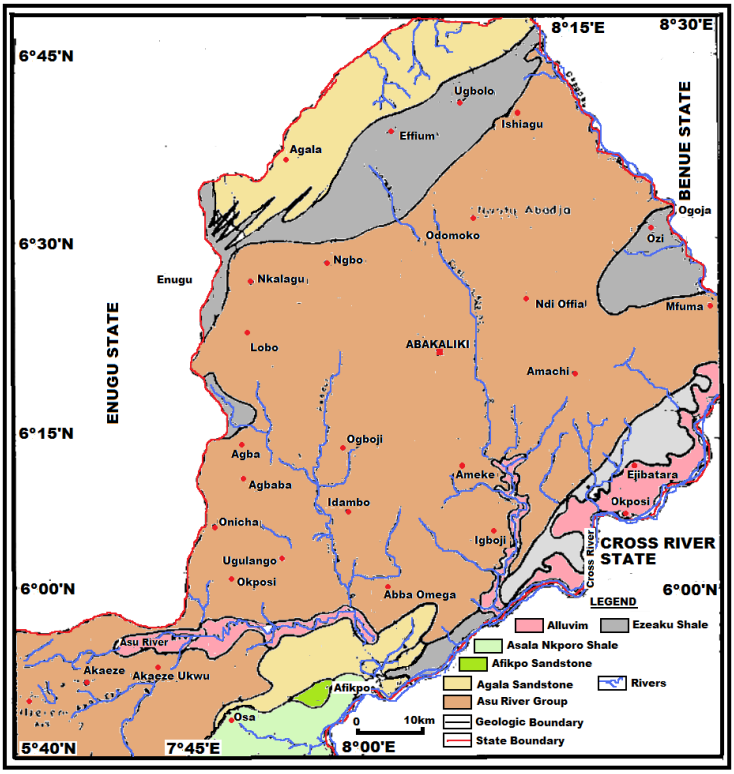

Figure no1: Regional geology map of the study area(Adapted from NGSA)

Piper Diagram

This is a graphical representation of the chemistry of a water sample or samples. The cations and anions are shown by separate ternary plots. The apexes of the cation plot are calcium, magnesium and sodium plus potassium cations. The apexes of the anion plot are sulphate chloride and carbonate plus bicarbonate anions. The two ternary plot are then projected up into a diamond. The diamond is a matrix transformation of a graph of the anions and cations.

Stiff Diagrams

These are graphical representation of water chemical analyses first developed by H.A.Stiff in 1951. A polygonal shape is created from the three or four parallel horizontal axes extending on either side of a vertical zero axes. Cations are plotted in milliequivalent per litre on the left side of the zero axis one to each horizontal axis and anions are plotted on the right side.

Schoeller Diagram

Schoeller diagram is a semi-logarithmic diagram of the concentration of the main ionic constituents in water (SO_4, HCO_3, Cl, Mg, Ca, Na/K) in equivalent per million per kg of solution (meq/Kg). An equivalent is the amount of an anion or cation species needed to add or remove one mole of electrons from a system. The concentration of each ion in each sample are represented by points on six equally spaced lines and points are connected by a line. The diagram gives absolute concentration but the line also gives the ratio between two ions in the same sample.

II. Materials and Methods

For the purposes of interpretation using graphical methods, the following parameters were used: magnesium, calcium, potassium and sodium for the cations while the anions used include the following: carbonate, bicarbonate, sulphate, and chloride.Their values in milligram per litre were converted to milli-equivalent per litre and were further used generate Piper, Stiff, and Scholler diagrams. Plots of hydrochemical data on Piper, Stiff and Shoellerdiagrams revealed the distribution of chemical constituents (cations and anions) in groundwater within the the area. This was accomplished by using the Aqua-Chem Software version 1.4.2 (Rockware Corporation). Since the water samples from the study area were collected from various sections of the area with diverse geological formations, the interpretations were carried out along selected profiles. Eight profiles were used which include A-A', B-B', C-C', D-D', E-E', F-F', G-G' and H-H' as shown in figure 2 below.

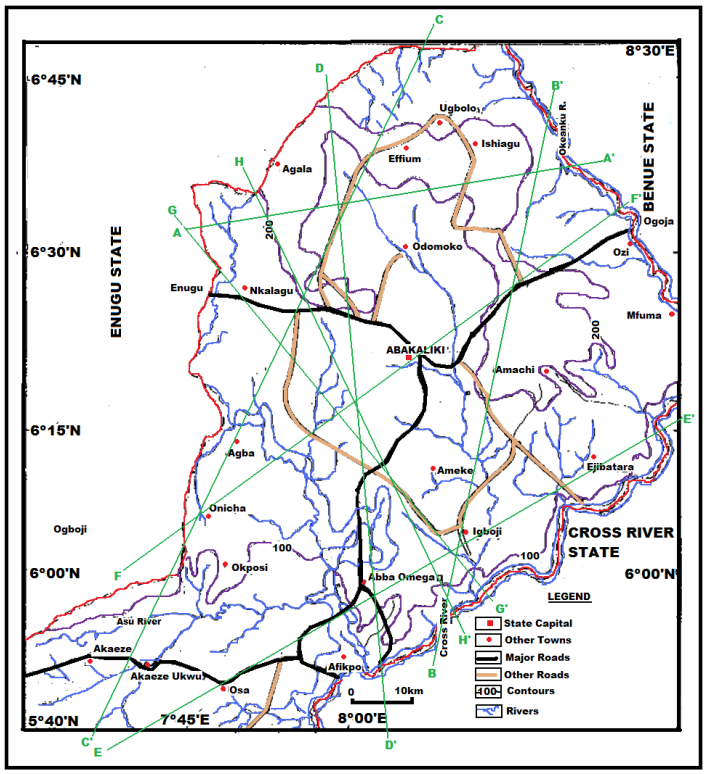

Figure no 2: Location/topography map of the study area showing the interpretative cross sections (profiles)

III. Results

The table below summarizes the geochemical resuts of the groundwater samples collected within the study area.

Table no 1. Summary of the results of the geochemical analysis of the study area

BH. Code	Calcium	Magnesium	Sodium	Potassium	Iron	Manganese	Copper	Sulphate	Chloride	Bicarbonate	Carbonate	Nitrate
B65	49	28.4	Nil	Nil	Nil	0.01	0.2	62	215	140	100.9	22.3
B46	98	27.2	2	0.6	0.02	0.016	Nil	50	145	60	25	38
B56	79	20.4	25.3	Nil	0.1	0.01	0.1	120.5	89.5	55.1	38.1	11.3
B58	86	3.6	52.9	Nil	0.1	0.01	0.02	78.2	76.2	65	55	7.2
B87	113	23.6	1.6	Nil	0.02	Nil	Nil	99.3	91	60	48.1	8.1
B70	108	Nil	169	Nil	0.02	0.01	0.001	140	102.1	52.1	48.9	7.5
B85	89	40.3	4.3	Nil	Nil	Nil	Nil	206.6	67.7	48	28	11
B96	38	0.3	72	Nil	0.12	0.02	Nil	137.4	84.1	85.1	60.2	7.1
B97	29	Nil	14	Nil	Nil	Nil	Nil	79	120.3	66.1	48.9	12.3
B84	74	0.74	8.3	0.3	0.02	0.02	Nil	296.4	87	43.9	25.1	12.1
B42	128	0.06	90	Nil	0.03	0.01	Nil	85	145	40	24	11.2
B39	64	33.3	75.44	Nil	0.13	0.01	Nil	190.3	109.1	61.1	43.6	8.4
B67	132	45.7	69	Nil	Nil	0.06	Nil	145	59.8	100.2	187.6	8.6
B43	69	13	0.05	Nil	Nil	0.02	0.02	126	119.2	128.5	85.2	11.1
B47	69	4	9.8	0.11	0.016	0.01	Nil	286	74.3	112	76	7.9
B22	120	41.8	35.2	Nil	Nil	0.013	Nil	450	65.7	106.3	84.1	8.2
B21	46.09	18.24	9	Nil	0.12	Nil	Nil	900	72	133	76.9	8
B31	56.12	17.02	8	Nil	0.12	Nil	Nil	230	79.1	93.1	45.8	7.1
B15	52.1	7.13	9	Nil	0.12	Nil	Nil	850	75	106	21	38
B30	38.08	26.75	11.5	Nil	0.06	Nil	Nil	600	62	121	87	10
B68	26.05	6.08	21	Nil	0.12	Nil	Nil	129.4	197	134.2	198.7	8.2
B24	56.8	17.2	9.2	Nil	0.14	Nil	Nil	150	192	42	20	12
B38	43.4	16.8	42.5	Nil	0.8	Nil	Nil	270	205	360	320	6.8
B53	26.05	6.28	62.4	Nil	0.12	Nil	Nil	406.1	180.2	184.7	105.3	6.6
B17	28.08	16.75	12.5	Nil	0.08	Nil	Nil	355.2	132	162.5	120.4	6.9
B83	59	15.4	86.5	Nil	1.8	Nil	Nil	230	124.1	203	169	7.6
B100	36.2	12.4	22.5	Nil	0.4	Nil	Nil	356.7	101.3	107.4	86.2	7.7
B61	62.4	14.5	48.6	Nil	0.7	Nil	Nil	365.8	179.6	130.3	87.3	7.1
B94	14.3	16.5	68	Nil	8	Nil	Nil	234.1	201.3	159.7	98.6	6.4
B55	38.42	12.62	48.5	Nil	0.45	Nil	Nil	135	308	51	20	7
B59	21	12	114	6.7	0.2	0.19	Nil	290.4	214.1	64.4	45.9	9.1
B90	24	12	128	6.6	0.18	0.12	Nil	507.8	107	55.2	45.2	8.2
B97	21	13	126	6.1	0.21	0.12	Nil	496.2	195.1	118.3	67.5	7.4
B81	24	14	21	7.9	0.2	0.1	Nil	750.1	159.2	89.5	64	7.3
B28	23	18	21	8	0.03	0.11	Nil	357.3	100.3	99.2	76.5	8.5
B79	222	30	29	Nil	0.01	0.01	Nil	450.4	239.3	88.2	57.5	8.4
B86	291	28	31	Nil	0.01	0.01	Nil	100.1	184.2	88.2	65.4	11.2
B48	304	Nil	64	Nil	0.02	0.02	Nil	65	50	45	26	6
B60	216	45	24	Nil	0.02	0.01	Nil	115	85	43	23	8
B63	140	63.9	63	1.04	0.033	0.1	Nil	96.9	204.3	89.2	78.9	6.8
B62	81	80.2	31	Nil	0.04	0.1	Nil	120	330	55	22	10.2
B99	185	116.98	121	6.8	0.2	0.02	Nil	103.1	150.7	102.9	89.9	7.8
B89	188	125.4	120	8	0.05	0.03	Nil	247.1	130.2	77.9	65	7.9

Results from the Piper trilinear plots.
The Piper plots for the 8 profiles are shown below.

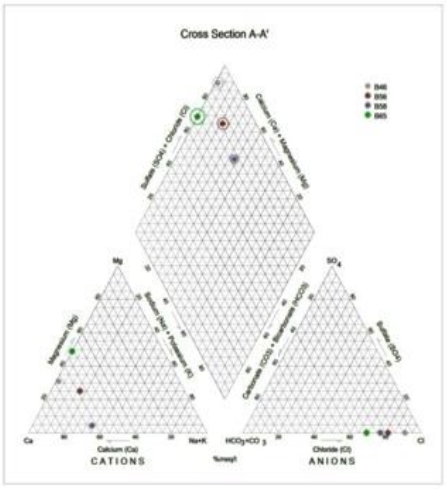

Figure no 3: Piper diagram interpretation along A-A' profile

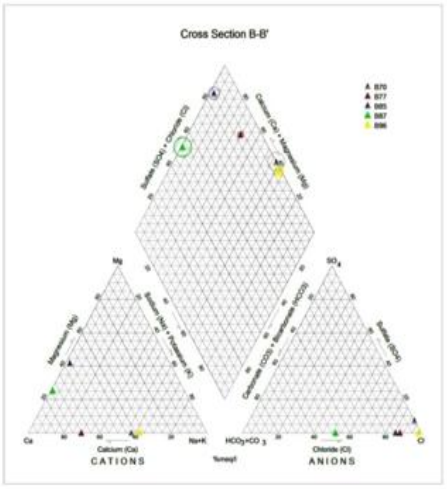

Figure no 4: Piper diagram interpretation along B-B'profile

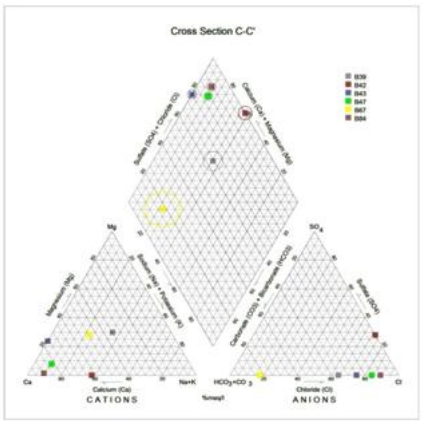

Figure no 5: Piper diagram interpretation along C-C' profile

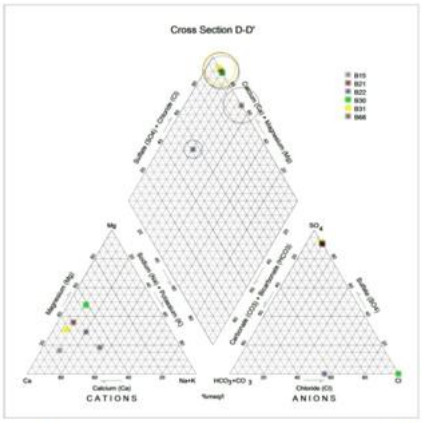

Figure no 6: Piper diagraminterpretation along D-D' profile

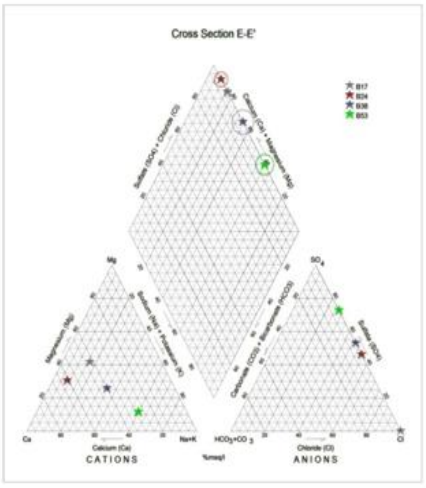

Figure no 7: Piper diagram interpretation along E-E' profile

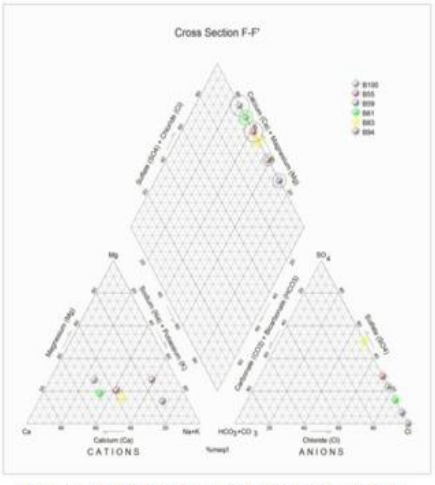

Figure no 8: Piper diagram interpretation along F-F' profile

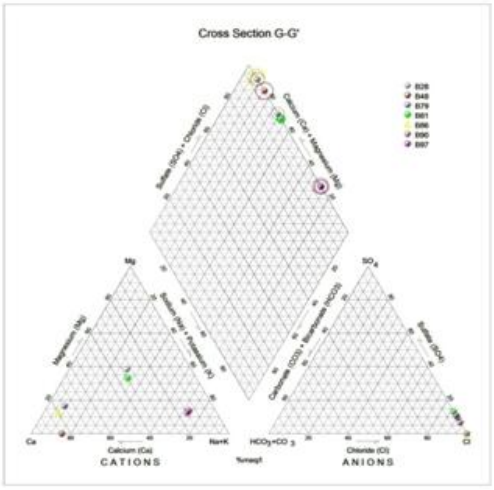

Figure no 9: Piper diagram interpretation along G-G' profile

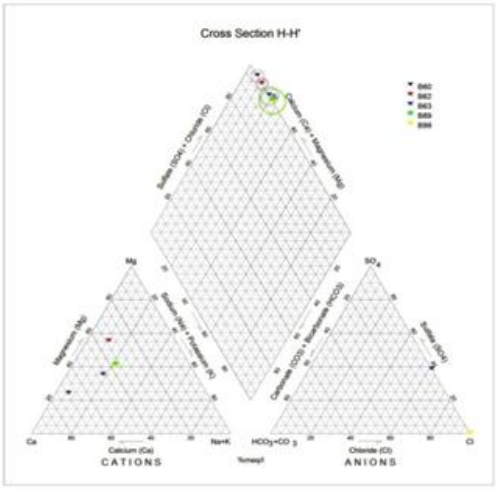

Figure no 10: Piper diagram interpretation along H-H' profile

Along the A-A' cross-section, the following boreholes were considered: B46,B56, B58 and B65. The Piper diagram revealed that the water class is of Ca-SO_4-Cl^- which is typical of gypsum ground waters and mine drainages. For B-B' profile, the following borehole samples were used in plotting the Piper diagram along this cross-section: B70, B77, B85, B87 and B96. The Piper diagram along this profile revealed a mainly Ca-Mg-SO_4-Cl^- water type. Six borehole samples were used for the plot along C-C' Profile. They include B39, B42, B43, B47, B67, and B84. Borehole sample B67 revealed groundwater that is believed to be fresh. However, the Piper diagram along this cross-section revealed two water types (hydrogeochemical facies) namely: Ca-SO_4-Cl^- (typical of gypsum groundwaters and mine drainage) and Ca-HCO_3^--CO_3 (indicating shallow fresh water aquifers). Only one borehole sample (B67) was revealed to be fresh along this cross-section.

For D-D' cross-section, boreholes B15, B21, B22, B30, B31 and B66 were used. The Piper plot revealed only one hydrogeochemical facies (water type), the Ca-Mg-SO_4^- type.

The borehole samples used for E-E' profile include B17, B24, B36, and B53. The Piper diagram revealed a water class of the Ca-Mg-SO_4^- type. For the F-F' cross-section, the following samples were used: B100, B55, B59, B61, B83 and B94. The water type revealed by the Piper diagram is indicative of Ca-Mg-$SO4^-$ and Na-Cl^- water types. The Na-Cl^- water type is typical of marine and deep ancient groundwaters. Borehole samples with this water type are very saline.

The borehole samples used for the G-G' profile include the following: B28, B48, B79, B81, B86, B90 and B97. Interpretation of the Piper diagram along this cross-section revealed a combination of two water types: the Ca-Mg-$SO4^-$ and Na-Cl^- water types. For the H-H' profile, borehole samples from B60, B62, B63, B89 and B99 were used. Interpretation of the Piper diagram along this profile revealed mainly Ca-Mg-$SO4^-$ water type (indicative of gypsum groundwater and mine drainage).

Results from Stiff Diagrams

The plots for the Stiff diagrams are shown in the figures below.

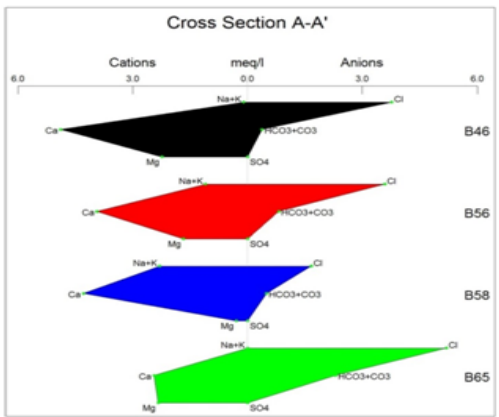

Figure no 11: Stiff diagram interpretation along A-A' profile

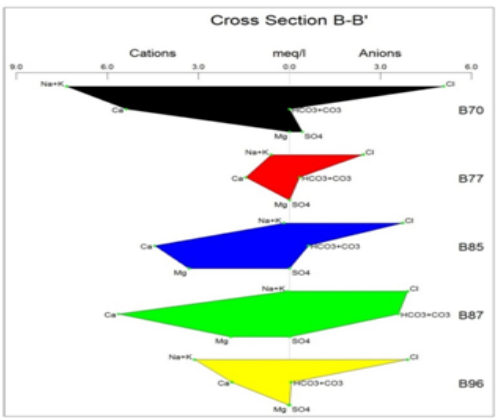

Figure no 12: Stiff diagram interpretation along B-B' profile

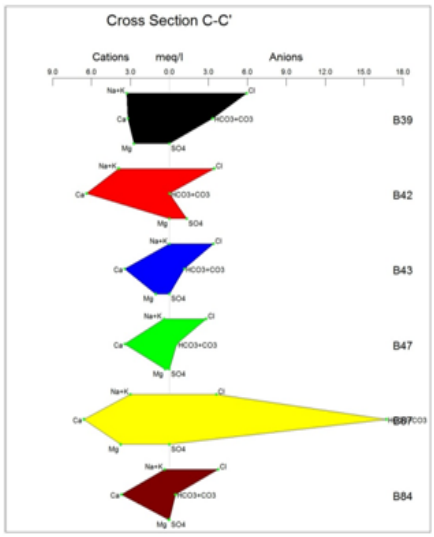

Figure no 13: Stiff diagram interpretation along C-C' profile

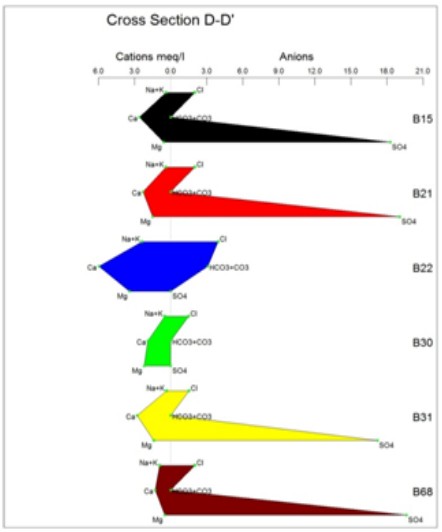

Figure no 14: Stiff diagram interpretation along D-D' profile

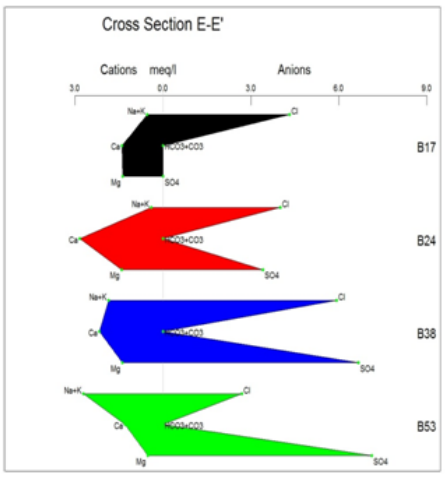

Figure no 15: Stiff diagram interpretation along E-E' profile

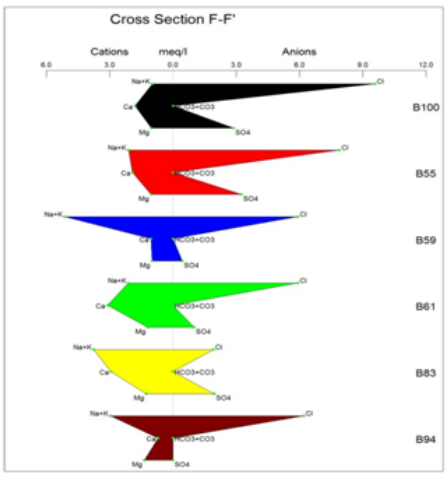

Figure no 16: Stiff diagram interpretation along F-F' profile

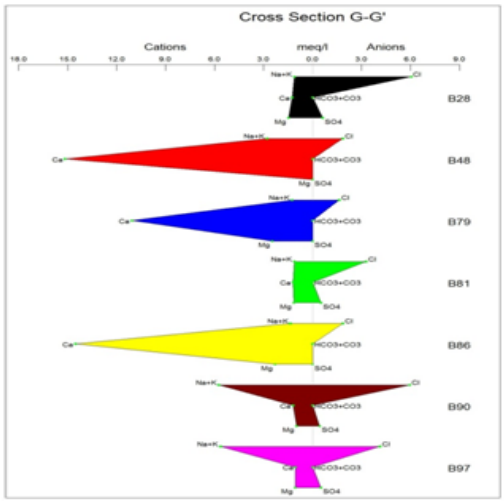

Figure no 17: Stiff diagram interpretation along G-G' profile

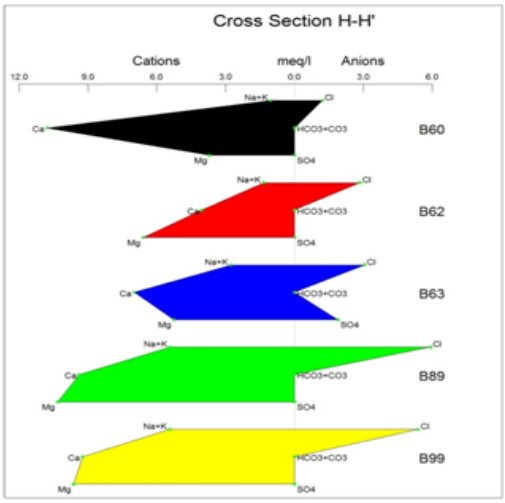

Figure no 18: Stiff diagram interpretation along H-H' profile

The Stiff diagram along A-A' profile revealed the following hydrogeochemical facies (water type): Ca-Mg-Cl^- type as revealed at borehole points B46, B56 and B65 and Ca- Na +K-Cl^- as revealed at borehole point B58. The different hydrogeochemical water types interpreted is based on the respective shapes of the different stiff plots. Similarly, borehole samples B46 and B56 revealed groundwater types from the same source and origin. In addition, based on the shapes of the Stiff diagrams, a great similarity was discovered to exist between the origins of the groundwater samples from B46 and B56 and to a lesser extent the B65 borehole sample.

Two water types were revealed from the B-B' profile**.** They include Ca-Na+K-Cl^- and Ca-Mg-Cl^- types.

Two major water types are revealed from the Stiff plot for C-C' profile. They include the following water types: Na+K-Ca-Cl^- and Ca-Mg-Cl^- . These water types are indicative of the geology and the residence time of the groundwater.

Interpretation of the Stiff plot along D-D' profile revealed a diversity of different hydro-geochemical facies indicating the various rock types and formations. The water types include the following: Na+K-Ca-Cl^- , Na+K-Ca-SO_4^-, Ca-Mg-Cl^- , and Ca-Mg-HCO_3^- .

For E-E' profile, the water types revealed include the following: Ca-Mg-Cl^- at borehole points B17 and B24. Other water types interpreted include Ca-Na+K-Cl^- and Na+K-Ca-SO_4^-. However, the dominant water types in this area are Ca-Mg-Cl^- and Ca-Na+K-Cl^- water types.

The hydrogeochemical facies interpreted along F-F' profile as revealed by the Stiff diagram include the following: Ca-Mg-Cl^- as revealed at borehole point (B100), Na+K-Ca-Cl^- at borehole point (B55), Na+K-Mg-Cl^- at borehole point (B59), and Na+K-Ca- SO_4^- at borehole point (B83). However, the dominant water types are Ca-Mg-Cl^- and Na+K-Mg-Cl^-.

Water types revealed along G-G' profile include the following: Mg-Ca-SO_4^-at borehole point B28 and B81, Ca-Na+K-Cl^- at borehole point B48, Ca-Mg-Cl^- at borehole point B79 and B86, and Na+K-Ca-Cl^- at borehole points B90 and B97. The dominant water types are Mg-Ca-SO_4^- , Ca-Na+K-Cl^- and Na+K-Ca-Cl^-. The Stiff plot also revealed that the groundwater types from borehole points B28 and B81 are from the same source. Similarly, from the shape of the Stiff plots, the water types from borehole points B48 and B79 have the same origin. Finally, the water samples from borehole points B90 and B97 are from the same source.

Water types interpreted from H-H' profile include the following: Ca-Mg-Cl^- at borehole point B60 and B63, while water type Mg-Ca-Cl^--SO_4^- was revealed at boreholes B62, B63 and B89. The dominant water type in the study area is mainly that of Mg-Ca-Cl^--SO_4^-. Similarly, borehole water samples from boreholes B89 and B99 are from the same source while groundwater samples from borehole points B62 and B63 are expected to have the same origin.

Results from Schoeller Diagrams

The Schoeller diagrams for the 8 interpreted profiles are shown below.

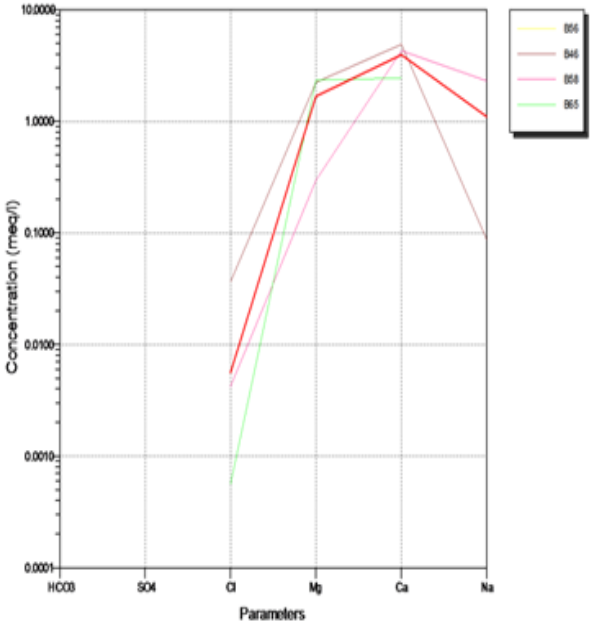

Figure no 19: Schoeller diagram interpretation along A-A' profile

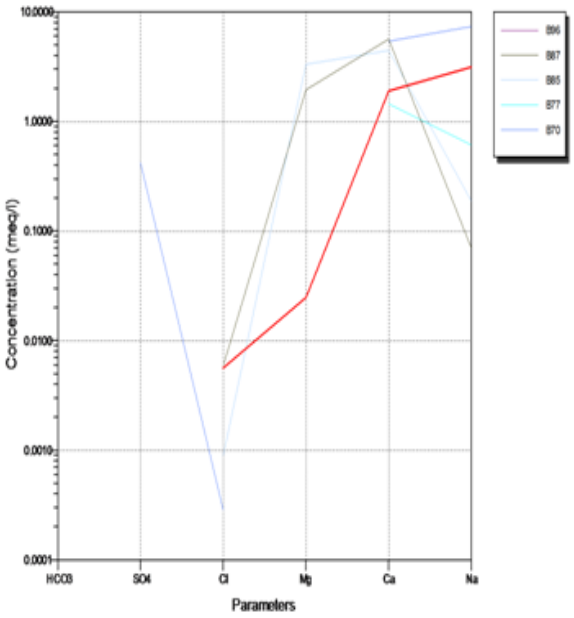

Figure no 20: Schoeller diagraminterpretation along B-B' profile

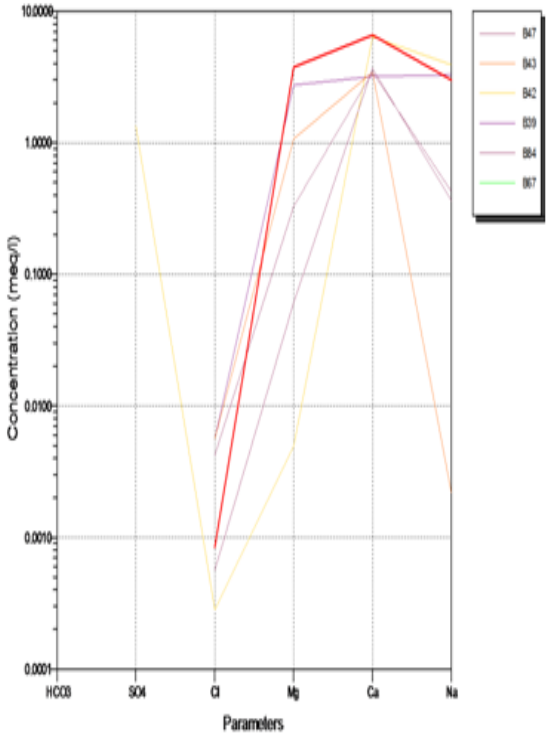

Figure no 21: Schoeller diagraminterpretation along C-C' profile

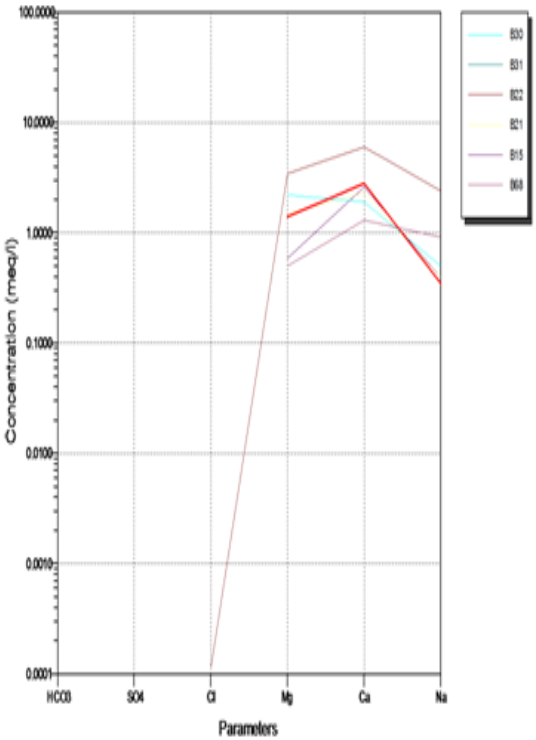

Figure no 22: Schoeller diagraminterpretation along D-D' profile

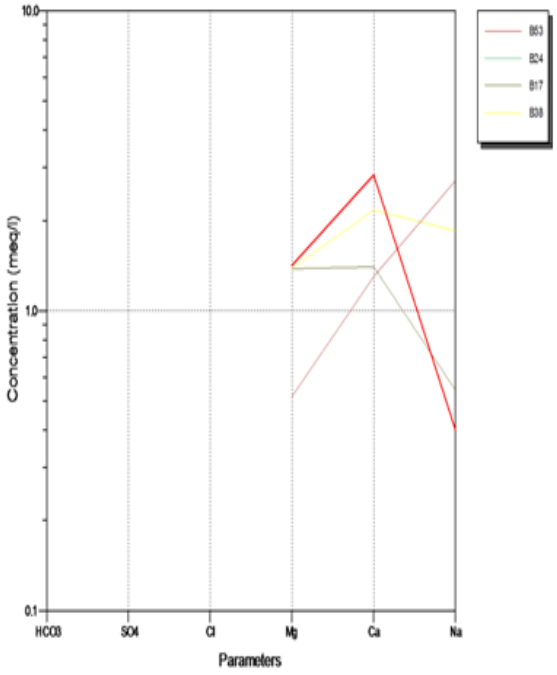

Figure no 23: Schoeller diagram interpretation along E-E' profile

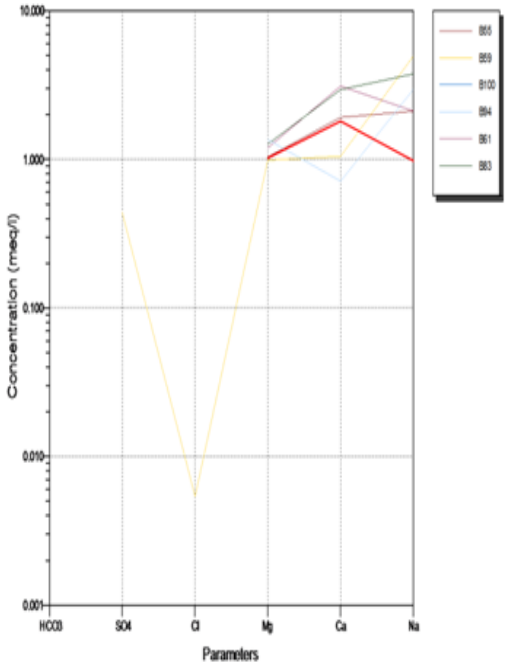

Figure no 24: Schoeller diagram interpretation along F-F' profile

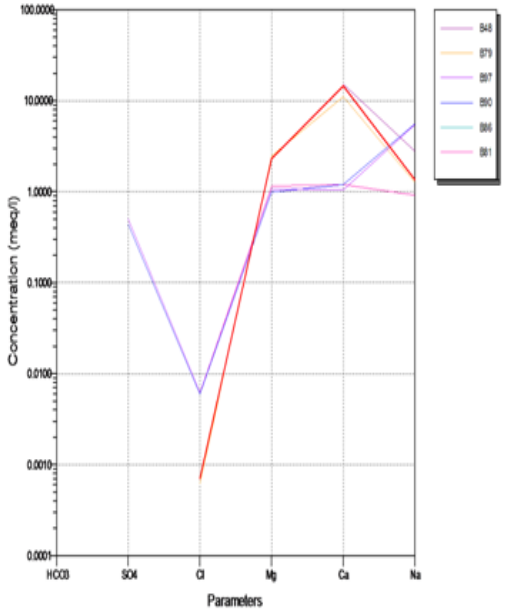

Figure no 25: Schoeller diagraminterpretation along G-G' profile

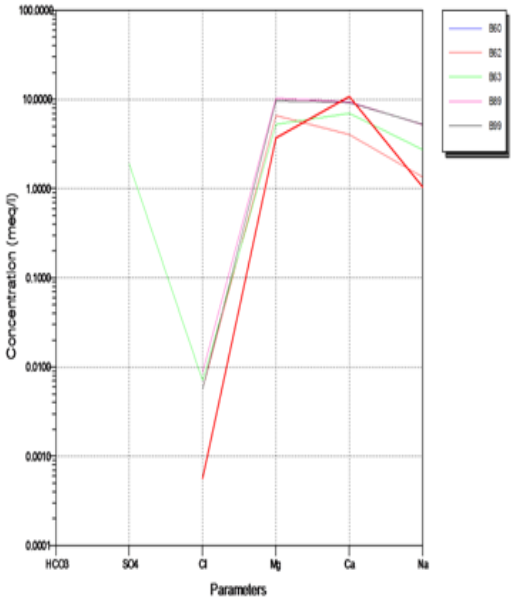

Figure no 26: Schoeller diagraminterpretation along H-H' profile

The hydrogeochemical facies identified along A-A' profile is mainly of the Ca-Na-Cl- water type.
Along B-B' profile, the Na-Ca-SO_4^- water type was interpreted.
The Ca-Na-SO_4^- water type was interpreted from C-C' profile.
The Ca-Mg-Cl^- water type was interpreted as the dominant hydrogeochemical facies from D-D' profile.
The Ca-Na-Cl^- water type is the dominant hydrogeochemical facies interpreted along the E-E' profile.
The Na-Ca-SO_4^- water typewas interpreted from the Schoeller diagram to be the most dominant water type along the F-F' profile.
Ca-Mg-SO_4 water type was interpreted as the dominant hydrogeochemical facies along G-G' and H-H' profiles.

IV. Discussion

The hydrogeochemical characteristics of the major and minor ions was carried out with a view to determining the groundwater types and visualizing trends of groundwater chemistry. Statistical distribution diagrams such as Piper trilinear diagram, etc were used to gain better insight into the hydrochemical processes operating in the groundwater system. The diagnostic chemical character of water solutions in hydrologic systems has been determined with the application of the concept of hydrochemical facies, which enables a convenient subdivision of water compositions by identifiable categories which reflects the effect of chemical processes occurring between the minerals within the subsurface rock units and the groundwater. Water types are often used in the characterization of waters as a diagnostic tool. From the plots, three different major water types were identified in the study area, viz: Na–K–Cl–SO_4–HCO_3, Na–K–HCO_3–Cl–SO_4 , and Na–Ca–Cl–SO_4–HCO_3^- water types. The water types tend towards sodium chloride bicarbonate which is consistent with expected water-rock interactions in such area. The result of this study reveals the following: First, it shows that groundwater in the watershed is of very different types which evolve from bicarbonate to chloride type. Secondly, large percentages of the samples fall within the Na-Cl category followed by Na-HCO_3 type. Thirdly, chloride is the dominant anion found in the groundwater in the study area. These water types would probably have resulted from precipitation of meteoric water through the different lithologic units (sand, shale granite gneiss, etc) in the area. Similarly, it is believed to be associated with the basinal brine of the Asu River Group. The Na^+ and K^+ may have resulted from silicate mineral weathering while Cl^- may have originated from evapotranspiration process, and HCO_3^- may be inorganic carbon ions produced when infiltrating water reacted with soil CO_2. The order of dominance of cations and anions is $Na^+ > K^+ > Ca^{2+} > Mg^{2+}$ and $HCO_3^- > Cl^- > SO_4^{2-}$ respectively. Generally, the chemical composition of groundwater is primarily dependent on the type of chemical reaction as well as the geochemical processes taking place within the groundwater system. Similarly, the mineralogical composition can exert an important control on the final water chemistry. As groundwater flows through the strata of different mineralogical composition, the water composition undergoes adjustments caused by imposition of new mineralogically controlled thermodynamic constraints.

Chloride is the most useful parameter for evaluating atmospheric input to water as it shows very little fractionation. Sodium and chloride inputs are likely to be mainly from rainfall and, therefore, will largely reflect the ratio observed in seawater. Cation exchange may account for a reduction in the Na concentration, and halite dissolution may account for high concentration of Cl. The low concentrations of potassium in natural water are a consequence of its tendency to be fixed by clay minerals and participate in the formation of secondary minerals. Dissolved species and their relations with each othercan reveal the origin of solutes and the processes that generated the observed composition of water. The Na/Cl relationship has often been used to identify the mechanism for salinity distribution and saline intrusions. The Na^+ and Ca^{2+} show a good correlation indicating that Cl^- and for the most part, Na^+ are probably derived from the dissolution of disseminated halite in fine-grained sediments. The high Na/Cl ratios are probably controlled by water rock interaction.When there is an exchange between Na^+ and K^+ in groundwater with Mg^{2+} or Ca^{2+} in the aquifer material, both of the indices are positive, indicating ion exchange of Na^+ in groundwater with Ca^{2+} or $Mg^{2+.}$ In general, these indices show positive values, whereas the low salt waters give negative values. The increase in groundwater salinity is usually accompanied by a slow rise in reverse ionic exchange,which indicates a cationic exchange that increases the hardness of these waters.The contribution of K^+ to the groundwater in these samples is modest. The low levels of potassium in water are a consequence of its tendency to be fixed by clay minerals and to participate in the formation of secondary minerals.

V. Conclusion

The graphical methods employed in the study have been useful in shedding more light on the groundwater chemistry, hydrogeochemical facies characteristics and origin of groundwater within the study area. The subdivisons of the water into groups with similar characteristics were useful in inferring the groundwater with similar geologic history and source.

References

[1]. Amajor LC. Aquifers in the Benin Formation (Miocene Recent), Eastern Niger Delta, Nigeria:Lithostratigraphy, Hydraulics, and Water Quality. Environ Geol Water Sci. 1991;17(2):85-101.
[2]. Edet AE, Okereke CS, Teme SC, Esu EO. Application of remote-sensing data to groundwater exploration: a case study of the Cross River State, south-eastern Nigeria. Hydrogeology Journal. 1998;6:394-404.
[3]. Edet AE, Okereke CS. Delineation of shallow groundwater aquifers in the coastal plain sands of Calabar area (Southern Nigeria) using surface resistivity and hydrogeological data. Journal of African Earth Sciences. 2002;35:433-443.
[4]. Esu OE, Okereke CS, Edet AE. A regional hydrostratigraphic study of Akwa Ibom State, South-eastern Nigeria. Global Journal of Pure and Applied Sciences. 1999;5(1):89-96.
[5]. Hem JD. Study and interpretation of the chemical characteristics of natural water. US Washington DC: Geological survey water supply. 1985;2254:263.

[6]. Hoque M. Pyroclastics from the Lower Benue Trough of Nigeria and their tectonicimplications. Jour. Afr. Earth Sci. 1984;2:351-358.
[7]. Olade MA. Evolution of Nigeria's Benue trough (Aulacogen): a tectonic model. GeologicalMagazine. 1975;112:575-583.
[8]. Olade MA. On the genesis of the lead-zinc deposits in Nigeria' Benue Rift (aulacogen): A re-interpretation.J. Min. Geol. 1976;13(2):20-27.
[9]. Ofoegbu CO. A review of the geology of the Benue Trough. Nig. J. Afr. Earth Sci. 1985;3:293-296.
[10]. Piper AM. A graphic procedure in the geochemical interpretation of water analysis. Am. Geophysics Union Trans. 1944;25:914-923.
[11]. Piper AM. A graphic procedure in the geochemical interpretation of water analysis. USGS groundwater note. 1953; no.12
[12]. Reyment RA. Aspects of the geology of Nigeria. Ibadan University press. 1965:133.
[13]. Uzuakpunwa BA. The Abakaliki pyroclastics, Eastern Nigeria: new age and tectonic implications. Geol. Mag. 1974;111:761-769
[14]. Whiteman AJ. Nigeria: its petroleum geology, resources and potential. Graham and Trotham, London. 1982;(I & II):394.

IOSR Journal of Applied Geology and Geophysics (IOSR-JAGG) is UGC approved Journal with Sl. No. 5021, Journal no. 49115.

Mgbeojedo T.I. "Inferring Groundwater Types From Graphical Methods: A Case Study of Afikpo And Abakaliki, South-Eastern Nigeria." IOSR Journal of Applied Geology and Geophysics (IOSR-JAGG) 6.5 (2018): 44-55.